Transdifferentiation of fibroblasts into muscle cells to constitute cultured meat with tunable intramuscular fat deposition

Tongtong Ma [1, 2, #], Ruimin Ren [1, 2, #], Jianqi Lv [1, #], Ruipeng Yang [1], Zheng Xinyi [1], Yang Hu [3], Guiyu Zhu [1], Heng Wang [1, *]

[1] College of Animal Science and Technology, Key Laboratory of Efficient Utilization of Non-Grain Feed Resources, Ministry of Agriculture and Rural Affairs, Shandong Agricultural University, Taian, China
[2] College of Animal Science and Technology, Huazhong Agricultural University, Wuhan, China
[3] College of Food Science and Technology, Huazhong Agricultural University, Wuhan, China
# These authors contributed equally to this work.
* Corresponding author: wangheng@sdau.edu.cn

Abstract

Current studies on cultured meat mainly focused on the muscle tissue reconstruction in vitro, but lack the formation of intramuscular fat which is a crucial factor in determining taste, texture and nutritional contents. Therefore, incorporating fat into cultured meat is of superior value. In this study, we employed the myogenic/lipogenic transdifferentiation of chicken fibroblasts in 3D to produce muscle mass and deposit fat into the same cells without the co-culture or mixture of different cells or fat substances. The immortalized chicken embryonic fibroblasts were implanted into the hydrogel scaffold and the cell proliferation and myogenic transdifferentiation were conducted in 3D to produce the whole-cut meat mimics. Compare to 2D, cells grown in 3D matrix showed elevated myogenesis and collagen production. We further induced fat deposition in the transdifferentiated muscle cells and the triglyceride content could be manipulated to match and exceed the levels of chicken meat. The gene expression analysis indicated that both lineage-specific and multi-functional signalings could contribute to the generation of muscle/fat matrix. Overall, we were able to precisely modulate muscle, fat, and extracellular matrix contents according to balanced or specialized meat preferences. These findings provide new avenues for customized cultured meat production with desired intramuscular fat contents that can be tailored to meet the diverse demands of consumers.

Introduction

Cultured meat is an innovative and emerging technique that produces meat directly from cell cultures, potentially providing a high-quality, safe, and stable source of animal protein (Chriki and Hocquette, 2020). In comparison to traditional livestock and poultry farming, cultured meat generates fewer greenhouse gases, utilizes less arable land, and causes less animal harm (Mattick et al., 2015). Proper selection of seed cells is one of the keys to the success of cultured meat production. The starting cells must be easily obtainable and be able to proliferate numerous times to enable mass production. While the stem cells like muscle stem cells and pluripotent stem cells have frequently been utilized as the cellular source for cultured meat, these stem cells are rare in the animal body and difficult to obtain and amplify on a large scale. In contrast, the somatic cells, which constitute the body, could be efficiently converted into muscle cells under certain conditions. The fibroblast is one of the most abundant and widely-distributed cell types present in the body and could be easily collected via minimally invasive biopsy procedure without sacrifice the farm animals. The fibroblasts can replicate indefinitely in vitro and are amenable for myogenesis, adipogenesis and chondrogenesis (French et al., 2004; Yin et al., 2010), which produce muscle, fat and extracellular matrix (ECM) proteins that constitute the meat and the associated texture and flavor. Recently, the fibroblast cells from farm animals have been utilized as the source cells for cultured meat production, with or without myogenesis (Jeong et al., 2022; Pasitka et al., 2023), demonstrating the feasibility of somatic cell-derived seed cells as a sustainable and ethical option for cultured meat production.

We have previously developed a protocol for the controlled transdifferentiation of chicken fibroblasts into myoblasts, which subsequently form multinucleated myotubes and express mature muscle proteins (Ren et al., 2022). Moreover, chicken fibroblasts could also be efficiently converted into fat-depositing lipocytes by treating them with chicken serum medium or other substances such as fatty acids (Hausman, 2012; Kim et al., 2020; Lee et al., 2021). Therefore, the induced myogenic and adipogenic competency, along with the inherent fibrogenic collagen-producing ability of chicken fibroblasts, can enable us to simultaneously synthesize muscle, fat and collagen during the cultured meat production. Nevertheless, further techno-functional research is necessary to precisely control the composition of the end product of fibroblast-derived cultured meat in order to achieve a more balanced and personalized nutritional profile and meet the specific consumer preferences.

In this study, the chicken fibroblast cells were implanted into the hydrogel scaffold to analyze the 3D cellular dynamics involving cell proliferation and myogenic/adipogenic transdifferentiation. We also optimized the low-serum culture conditions of chicken fibroblasts to reduce the cost of mass production. The myogenic transdifferentiated cells were confirmed to be skeletal muscle lineage but not myofibroblasts. Importantly, the cells were subjected to myogenesis and adipogenesis sequentially in 3D hydrogel matrix to resemble the whole-cut meat with the controllable intramuscular fat and collagen content. By using transdifferentiation strategies, the depositing ratio of fat into the cultured meat could be manually and precisely adjusted, allowing the nutrients to be naturally synthesized from the organized muscle structure. This demonstrates the potential for manipulating cultured meat to meet consumer preferences for specific fat content and texture.

Results

Chicken fibroblasts proliferate stably in low-serum conditions

The chicken fibroblast cells were chosen as the ideal cell source for cultured meat production because they can propagate indefinitely and undergo myogenesis whenever the induction is provided. These cells can be readily obtained from fertilized eggs without the need to harvest animals. We have previously constructed an inducible myogenic transdifferentiation system in chicken fibroblasts with the stable integration of Tet-On-MyoD cassette (Ren et al., 2022). The MyoD is the key myogenic transcription factor and the chicken fibroblasts could be converted into striated and elongated myotubes (myofibers) upon forced expression of MyoD (Ren et al., 2022; Weintraub et al., 1989). The Tet-On-MyoD cassette enables the inducible and reversible activation of chicken MyoD factor, and in the current fibroblast cells, the myogenic transdifferentiation is only switched on by adding doxycycline (DOX). Without the DOX treatment, the control chicken fibroblast cells (Tet-On-MyoD) do not differ from the wild-type cells in terms of morphology, proliferation rate and gene expression (Figure S1A, S1B, S1C). Hence, as a proof-of-concept experiment, we utilized this inducible myogenic fibroblast cell line to develop protocols for cultured chicken meat production.

To achieve sustainable and cost-effective cell production, it is essential to minimize the serum usage in the culture medium. Therefore, we implemented a progressive serum reduction approach to acclimate the cells in the prospect of obtaining a stable cell source

that can be propagated in low serum concentrations. In the initial experiment, we used 12% fetal bovine serum (FBS) in 1640 basal medium, which served as the control group. The results showed that the cells were able to proliferate normally at 6%, 3% and 1.5% serum concentrations, but at decreasing rates as shown by the EdU assay (Figure 1A and 1B). We also tested the chicken serum as an alternative to bovine serum, in order to avoid cross-species contamination of animal derivatives. The results showed that chicken fibroblasts could proliferate stably in the 1% chicken serum (Figure 1A, 1B, S1D) and the cell populations multiply 3 times in 3 days as demonstrated by the CCK-8 assay (Figure 1C). Thus, we conclude that the low-serum medium can effectively support the stable propagation of chicken fibroblasts.

3D culture of chicken fibroblasts in GelMA hydrogels

The behavior of cells grown on the top of 2D flat surface may differ from that of cells in 3D space. To simulate the 3D natural growth environment of cells *in vivo*, we utilized the Gelatin Methacrylate (GelMA)-based hydrogels as scaffolds for chicken fibroblasts. GelMA hydrogel can form a stable and porous structure for cell implantation and is commonly used in tissue engineering because of its great biocompatibility and mechanical tenability (Pepelanova et al., 2018). We created hydrogels with varying concentrations at 3%, 5%, 7%, 9%, and then observed their surface characteristics when immersed in culture medium using an emission scanning electron microscope. The porosity was measured to be 83.27%, 65.01%, 62.47% and 57.96%, respectively. Thus, the higher the mass concentration of hydrogels, the tighter the 3D mesh structure formed and the smaller the porosity (Figure 2A). The pore diameters in the scaffolds were determined to range from 3μm^2 to 100μm^2, showing the biggest pore size in 3% hydrogel and smallest in 9% hydrogel (Figure 2B). Therefore, the porosity and pore size of the scaffold could be adjusted to achieve optimal physical strength and nutrients delivery that suited for long-term cell culturation.

To determine the most ideal gel concentration and pore size suited for chicken fibroblast attachment and growth, we conducted an experiment where we implanted the same number of cells into gels with varied pore sizes and examined the cellular dynamics over a 9-day period (Figure S2). The cells adhered to the gels immediately and started to exhibit typical extended and irregular fibroblast cell morphology after 1 day, indicating the hydrogel's good biological compatibility with chicken fibroblast cells. However, the 3% hydrogel collapsed in the medium 2 days after cell implantation and

126 thus did not support the long-term cell growth. We continued to monitor the 3D cell
127 proliferation and found that the cells successfully propagated in 5%, 7%, 9% hydrogels
128 for the entire duration of the experiment. Among the tested hydrogels, the 5%
129 concentration was found to be the best option for cell attachment and growth as shown
130 by the densest cellular structure formed, and thus be utilized for the subsequent analysis.
131
132 Due to the challenges of observing and distinguishing the cells and pores within the
133 hydrogel scaffold using the brightfield of ordinary light microscopy, we then used the
134 PKH26 fluorescent cellular dye to accurately observe the cellular morphology and
135 quantity the cell numbers. The cells were firstly labelled with PKH26 in 2D culture
136 (Figure S3A) and then transferred into the gel matrix. Upon implantation, the cells
137 appeared mostly round on the first day, but gradually extended and expanded within the
138 hydrogel scaffold. By the 5th day, most of the cells were elongated with irregular shape
139 and short tentacles and packed tightly, and by the 9th day they multiplied more than 15
140 times and formed dense fibrous bundles (Figure 2C and 2D). We also examined the
141 proliferation dynamics of the cells in 3D scaffold via the EdU assay. The proliferation
142 efficiency of chicken fibroblast cells gradually increased overtime in 3D culture and
143 reached replication levels even higher than those in 2D culture (Figure 2E and 2F). This
144 result indicates that 3D culture conditions provide a more favorable environment for
145 cell growth. Moreover, when the 3D cultured cells were detached from the gel by
146 collagenase dissociation (Figure S3B) and seeded back in 2D monolayer culture plates,
147 the cells again exhibited similar morphology but slightly increased proliferation
148 capacity compared to the original fibroblasts in 2D conditions (Figure S3C and S3D).
149 Thus, the chicken fibroblast cells cultured in 3D maintain their normal physiological
150 characteristics and we continue to stimulate the cellular myogenesis and lipogenesis to
151 prepare them for cultured meat production.
152
153 **Transdifferentiation of chicken fibroblasts into muscle cells in 3D**
154 Despite the complexity in the composition of fresh meat and processed products,
155 muscle cells are the major and indispensable component of meat foods. The muscle cell
156 derived myotubes (myofibers) provide a rich source of proteins and nutrients and
157 constitute the meat texture. To this end, we aimed to transform the chicken fibroblast
158 into muscle cells through the established MyoD overexpression protocol (Ren et al.,
159 2022). We first tested and optimized the myogenic transdifferentiation parameters in
160 2D culture through the DOX induced MyoD expression (Figure S4). We observed

elongated multinucleated myotubes and abundant expression of myosin heavy chain (MHC) after 3 days of myogenic induction (Figure S5A). The "serum deprivation" protocol was the classical strategy to stimulate terminal myogenic differentiation in myoblasts of various species including chicken (Nakashima et al., 2005). Thus, we examined the myogenic transdifferentiation efficiency (myotube fusion index) in the chicken fibroblast cells overexpressing MyoD in combination with reduced concentrations of bovine or horse serums. However, we found that reducing serum concentrations did not increase the myotube formation but instead caused massive cell death instead (Figure S5B). Therefore, it seems that the "serum deprivation" could not further improve the myogenic transdifferentiation in chicken fibroblast cells and a simple MyoD overexpression strategy is sufficient for efficient production of mature muscle cells.

After demonstrating the feasibility of induced transdifferentiation of chicken fibroblasts into muscle cells in 2D culture, we continued myogenic transdifferentiation in 3D to simulate the construction of concrete whole-cut meat. The cells were inoculated into a hydrogel scaffold and allowed to proliferate for 7 days before inducing transdifferentiation with MyoD overexpression (Figure 3A). We used whole-amount MHC immunofluorescence staining to examine the myotube formation directly inside the gel. We identified abundant multinucleate MHC^{+} myotubes at multiple focal planes within the gel (Figure 3B, Supplementary Video 1), indicating successful myogenic transdifferentiation of 3D cultured chicken fibroblasts. In contrast, there were no MHC signal or autofluorescence detected in the 3D cultured chicken fibroblasts (Figure S5C) and hydrogel without cells (Figure S5D). With the assistance of confocal Z-stack analysis, the stacked images showed densely packed MHC+ myotubes from a piece of cellular hydrogel complex at a depth of 68 μm (Figure 3D). The separate XY axis views of the orthogonal projections at different depths (Figure 3E) and a multi-angle video (Supplementary Video 2) also showed the several myotubes were aligned together. Nevertheless, many myotubes were oriented in different directions, preventing the entire matrix from aligning in one direction. In conclusion, we successfully transformed the chicken fibroblast cells into mature muscle cells in 3D environment.

Compared to 2D, the transdifferentiated myotubes induced in 3D were more organized and densely packed, resembling the native myofiber distribution *in vivo* (Figure 3B). And the myotube formation efficiency (fusion index) in 3D reached 30.49%, which was

196 significantly higher than that of the 2D under the same transdifferentiation conditions
197 (Figure 3C). We also evaluated the expression of several myogenic markers by RT-
198 qPCR (Figure 3F). MyoG (Myogenin) is a transcription factor regulating terminal
199 skeletal muscle differentiation and could be induced by MyoD (Cao et al., 2006).
200 MYH6 (Myosin Heavy Chain 6) is the major protein comprising the muscle thick
201 filament, and functions in muscle contraction (van Rooij et al., 2009; Warkman et al.,
202 2012). MCK (Muscle Creatine Kinase) is an enzyme that primarily active in mature
203 skeletal and heart muscle (Vincent et al., 1993). All myogenic factors, including MyoG,
204 MYH6, and MCK, significantly increased upon transdifferentiation in both 2D and 3D.
205 In addition, the transdifferentiated cells exhibited significant higher expression of
206 MyoG and MCK in 3D conditions compared to that in 2D, indicating more robust
207 myogenic differentiation and maturation of cells in the 3D microenvironment. We
208 speculate that the porous structure of the hydrogel matrix may support the cells to grow
209 in all directions, similar to the environment in which the myofibers form in vivo.
210
211 Macroscopically, the muscle filaments and the dense cellular network structures formed
212 by myogenic transdifferentiation could make the hydrogel matrix more compact and
213 solid (Figure 3G). Thus, compared to the empty transparent scaffolds without cells, the
214 hydrogels cultivated with muscle cells are more visually like whole-cut meat thus
215 resemble to the fresh animal meat.
216
217 **Myogenic transdifferentiation of fibroblast does not produce myofibroblasts**
218 Fibroblasts can be induced to differentiate into myofibroblast upon injury, leading to
219 tissue fibrosis. Similar to the skeletal muscle cells, the myofibroblast are also contractile
220 and express the myogenic factor MyoD as well as certain types of sarcomeric myosin
221 heavy chains (MHC) (Hecker et al., 2011). To confirm that the myogenic
222 transdifferentiated cells were indeed skeletal muscle cells but not the myofibroblasts,
223 we utilized a panel of cell lineage-specific markers to delineate the cell conversion
224 progress and determine the cellular identity of fibroblasts, myoblasts and
225 myofibroblasts, respectively. The immunofluorescence staining of 3D cultured cells
226 showed that the muscle-specific intermediate filament Desmin (Paulin and Li, 2004)
227 was expressed only in the MyoD transdifferentiated cells, but not in the original
228 fibroblasts or the embryonic skin derived myofibroblasts (Figure 4A). In contrast, the
229 classical myofibroblast marker alpha-smooth muscle actin (α-SMA) (Hinz et al., 2007;
230 Takase et al., 1988) was expressed only in myofibroblasts, but not in the fibroblast or

231 the transdifferentiated cells (Figure 4B). The fibroblast intermediate filament Vimentin
232 (Tarbit et al., 2019) was abundantly expressed in the fibroblasts but reduced in the
233 myogenic transdifferentiated cells (Figure 4C). The 2D and 3D cultured cells showed
234 consistent pattern of marker protein expression, indicating that the different culture
235 models and conditions do not affect the cell identity conversion (Figure S6A and S6B).
236 These results confirmed that the MyoD indeed transdifferentiate the cells toward the
237 skeletal muscle lineage but not the myofibroblast. Furthermore, the RT-qPCR showed
238 that, after myogenic induction in 3D, the skeletal muscle specific genes Desmin and
239 Six1 (Relaix et al., 2013) were significantly elevated (Figure 4D) whereas the fibroblast
240 gene Thy-1 was significantly reduced (Figure 4E). The transforming growth factor β
241 (TGFβ) signaling is the most potent known inducer of myofibroblast differentiation
242 (Vaughan et al., 2000). We found the expression of core TGFβ signaling components,
243 TGFβ-1, TGFβ-3 and Smad3, remain unchanged during the transdifferentiation process
244 (Figure 4F), indicating that the classical myofibroblast lineage was not induced.
245 Together, these data confirm that the myogenic transdifferentiation of fibroblast does
246 not produce myofibroblasts.
247
248 **Stimulate the fat deposition in chicken fibroblasts in 3D**
249 The intramuscular fat is a crucial component of meat that can determine its quality
250 attributes, such as taste and flavor. The chicken fibroblasts have been reported to be
251 amenable for lipogenesis through various stimulus, including chicken serum, insulin,
252 fatty acids and retinoic acids (Kim et al., 2021; Kim et al., 2020; Lee et al., 2021). We
253 first attempted different lipogenic stimulations on 2D cultured cells and stained them
254 for Oil Red O to visualize and quantify fat deposition in the fibroblasts. Only very few
255 scattered Oil Red O signals were found in the treatments consisting of only serums
256 (12.5% FBS, 1% chicken serum or 2% chicken serum), indicating no lipogenesis during
257 normal proliferation conditions. However, when we added insulin and fatty acids
258 (oleic/linoleic acid) to the medium, lipid droplets in the cells dramatically increased as
259 detected by the Oil Red O staining. After extensive optimization of the concentrations
260 of supplements in the medium, we identified that the 8μg/ml fatty acids plus 60μg/ml
261 insulin (abbreviated as FI, F: fatty acids, I: insulin) can induce lipogenesis most
262 efficiently in 2D chicken fibroblasts (Figure S7A, S7B and S7C).
263
264 Next, the same lipogenesis induction strategy was applied to the 3D cultured cells
265 (Figure 5A). We found extensive Oil Red O signal inside the hydrogel matrix at

266 different focal planes and the lipid droplets were clearly visible as beaded strings under
267 magnification (5B and 5C, Supplementary Video 3). The RT-qPCR analysis illustrated
268 the expression of genes involved in lipogenesis and triglyceride synthesis were
269 significantly higher in the cells with lipogenic stimulation compare to the control
270 (Figure 5D). Notably, the genes encoding for PPARγ (peroxisome proliferator-activated
271 receptor gamma), Gpd1 (glycerol-3-phosphate dehydrogenase) and FABP4 (fatty acid
272 binding protein 4) all showed higher expression in 3D than that in 2D. Interestingly, the
273 expression of Znf423 (zinc finger protein 423), which is a PPARγ transcriptional
274 activator (Addison et al., 2014; Longo et al., 2018), only increased upon lipogenic
275 induction in 3D but not in 2D conditions. It seems that the cells grown in 3D hydrogel
276 showed enhanced lipogenesis compare to the flat surface cultured cells, similar to the
277 myogenic transdifferentiation process in 3D. In addition to the lipogenic induction with
278 fatty acids and insulin (FI), we also validated the use of chicken serum in promoting
279 lipid accumulation as previous reported (Kim et al., 2021). Our results showed that the
280 chicken serum alone could also stimulate fat accumulation effectively (Figure S7D, S7E
281 and S7F). We further measured the triglyceride content and found that the lipogenic
282 induction increased the triglyceride significantly in the cell matrix (Figure 5E). In
283 conclusion, the 3D cultured chicken fibroblast can efficiently deposit lipid by different
284 stimulus.
285
286 **Controlled fat deposition in the transdifferentiated muscle cells in 3D hydrogel**
287 The above presented data shows that chicken fibroblast cells have a superior capacity
288 for transforming into muscle and depositing fat when cultured in a 3D hydrogel matrix.
289 Next, we tried to combine the myogenic and lipogenic stimuli together to modulate the
290 fat deposition in the cultured meat to simulate the various intramuscular fat contents in
291 the conventionally raised meat. Rather than converting fibroblasts into muscle cells and
292 fat cells separately and mixing them later, we adopted a new strategy that can induce
293 de novo lipid deposition in the muscle by first inducing myogenic transdifferentiation
294 and then followed by lipid induction in the same cells (Figure 6A and S8A). In 2D
295 conditions, plenty of MHC^{+} myotubes and Oil Red O-stained lipids were found to
296 intermingle after the myogenic/lipogenic treatment (Figure S8B) and some of the red
297 marked lipid droplets were located inside the myotubes, indicating that the transformed
298 muscle cells indeed deposit fat autonomously to constitute intramyocellular lipids
299 (Figure S8C). Next, we applied the similar treatment to the cells cultured in 3D hydrogel
300 and also identified Oil Red O-labelled lipid droplets mixed with the densely packed

301 MHC^+ myotubes (Figure 6B and 6C). These findings suggest that the use of
302 myogenic/lipogenic treatments can induce the formation of muscle cells that are
303 capable of depositing fat in both 2D and 3D. We further examined the expression levels
304 of both myogenic and lipogenic factors in the 3D cultured cells by RT-qPCR. Compare
305 to the control 3D cells without myogenic/lipogenic stimulations, the induced cells
306 showed significantly higher expression of genes involved in both myogenesis and
307 lipogenesis (Figure 6D). Interestingly, the extent of gene upregulation upon the
308 combined myogenic/adipogenic stimulations was comparable to that of myogenic or
309 adipogenic induction alone. This finding suggests that sequential myogenic
310 transdifferentiation and lipid deposition do not interfere with each other when
311 conducted in the same cells.
312
313 The intramuscular fat is an integral component of both the traditional animal meat and
314 the cultured meat, and it directly influences the meat flavor and texture (Frank et al.,
315 2016). Hence, we compared the triglyceride levels in the 3D hydrogel cells with
316 different types of lipogenic stimuli with the chicken breast and leg meat. The results
317 showed that the lipogenic stimulation in the 3D hydrogel cells increased the triglyceride
318 content in the cultured meat to the levels comparable or even higher than real chicken
319 meat (Figure 6E). In contrast, the control cells without any induction or with only
320 myogenic stimulation do not show apparent triglyceride accumulation (Figure 6E).
321 Therefore, the fat content in the cultured meat could be synthesized by a controlled
322 manner and then we tried to purposely manipulate the triglyceride contents in the meat
323 matrix by adjusting the potency of adipogenic stimulation. By fine-tuning the
324 concentrations of insulin and fatty acids during lipogenic induction, the triglyceride
325 contents in the final product of cultured meat can precisely reach any customized levels
326 across the range from 1.5mg/g to 7mg/g (Figure 6E), which overlap and surpass the
327 levels in the fresh chicken breast and leg meat. As a result, this strategy greatly expands
328 the diversity and category of cultured meat products, allowing for precise control over
329 intramuscular fat contents to meet consumer preferences. Therefore, guided and graded
330 fat deposition in cultured meat allows for the creation of various meat products with
331 controlled intramuscular fat contents.
332
333 **The collagen content and ECM components of cultured meat**
334 Fibroblasts are an essential source of extracellular matrix (ECM) including the collagen,
335 which providing elasticity to the tissue in the body and enriching the texture of the

336 cultured meat (Ben-Arye and Levenberg, 2019). In theory, the fibroblast should produce
337 abundant ECM to produce a more realistic meat product. We then examined the
338 collagen content in the cultured meat and found that the total collagen protein gradually
339 increased and reached the plateau at 1.59 μg/mg in the final product (Figure 7A). This
340 is mainly due to the increased cell numbers and the accumulation of secreted collagen
341 in the hydrogel matrix. Nevertheless, the RT-qPCR showed that the genes encoding the
342 major components of ECM exhibited various expression patterns with the extension of
343 culture time. The expression of COL1A1 (Collagen, type I, alpha 1) and COL1A2
344 (Collagen, type I, alpha 2) gradually decreased, whereas the fibronectin increased
345 during the time course of meat synthesis. The expression of elastin and laminin genes
346 remain stable throughout the whole course of experiment (Figure 7B). However, the
347 laminin protein content was accumulated and increased steadily during 3D culturation
348 (Figure 7C). Overall, the synthesis and accumulation of different types and amounts of
349 ECM components during the myogenic/lipogenic stimulations can improve the texture
350 of the cultured meat prepared from fibroblast cells.

351 **The characterization of molecular changes during myogenic transdifferentiation**
352 **and fat deposition in cultured meat**

353 To provide insights into the functional shifts during the transdifferentiation from
354 fibroblasts toward muscle, fat, or muscle/fat cells in 3D culture, we further analyzed
355 the transcriptomes from the different populations of cells including the "original
356 fibroblasts" (3D_fibroblast), "myogenic transdifferentiated cells" (3D_MyoD),
357 "adipogenic transdifferentiated cells" (3D+FI), and "myogenic/adipogenic
358 transdifferentiated cells" (3D_MyoD+FI) (Figure 8A). To illustrate the relationship
359 between these cell groups, we conducted unsupervised hierarchical clustering analysis
360 of the entire transcriptome. The findings revealed that the 3D+FI group clustered
361 distinctly from the others, while the 3D_MyoD and 3D_MyoD+FI groups exhibited
362 greater similarity. Moreover, the 3D_fibroblasts formed a distinct sub-cluster on their
363 own (Figure 8B), suggesting that myogenic or adipogenic transdifferentiation drive
364 these cells away from their original fibroblastic state. The Principle Component
365 Analysis (PCA) of the transcriptomes also showed that distinct trajectories of myogenic
366 and adipogenic transdifferentiation routes were derived from the original fibroblasts
367 and finally integrated together into the myogenic/adipogenic cells (3D) (Figure 8C). It
368 indicates that the myogenic and adipogenic signalings could operate simultaneously
369 and separately during the generation of the culture meat composed of muscle and fat.

We also compared the differentially expressed genes (DEG) from “3D_MyoD vs 3D_fibroblast”, “3D+FI vs 3D_fibroblast” and “3D_MyoD+FI vs 3D_fibroblast”. The results showed that majority (78%) of DEGs in the 3D_MyoD+FI are overlapped with 3D_MyoD and 3D+FI, indicating that sequential myogenic/adipogenic induction in 3D_MyoD+FI is consistent with myogenic or adipogenic function individually (Figure 8D). The heat map also highlighted the representative myogenic or adipogenic genes that were upregulated in the myogenic, adipogenic, or myogenic/adipogenic cells constitute the culture meat. In contrast, the fibroblast genes were diminished during the transdifferentiation, confirming the loss of fibroblast identity (Figure 8E). In addition, the Gene Ontology (GO) analysis of up-regulated differentially expressed genes (DEGs) in 3D_MyoD+FI cells confirmed that myogenic-specific pathways such as “muscle organ development” and adipogenic-specific pathways such as “PPAR signaling pathway” were enriched. In addition, we also identified several multifunctional signaling pathways such as “JAK-STAT signaling pathway”, “NF-kappa B signaling pathway”, “MAPK signaling pathway” were simultaneously activated during myogenic/adipogenic transdifferentiation, which should have profound effects on both myogenesis(Bakkar and Guttridge, 2010; Jang and Baik, 2013; Keren et al., 2006) and adipogensis (Batista et al., 2012; Bost et al., 2005; Richard and Stephens, 2011) (Figure 8F). The upregulated genes in the representative pathways (such as “*Stat1*” in JAK-STAT signaling pathway, “*Mapkapk3*” in MAPK signaling pathway) were shown in (Figure 8G). In conclusion, the transcriptome analysis of the different types of transdifferentiated cells revealed not only the myogenic- and adipogenic-specific pathways driving the muscle formation and fat deposition respectively, but also several key multifunctional signaling pathways that can promote the cell fate transition and differentiation in different cellular contexts including the muscle and fat tissues.

Discussion

Mature muscle tissue primarily consists of myofibers (myotubes), which are long, multinucleated cells that contract to generate force and movement. In addition to myofibers, muscle tissue contains a variety of other cell types, including fibroblasts and adipocytes, all of which play important roles in the structure and function of the tissue. The extracellular matrix, which is mainly secreted by fibroblast cells, provides support and structural integrity to the muscle tissue. It is made up of a complex network of proteins and molecules, such as collagen, that provide a scaffold for the cells to attach to and interact with (Franco-Barraza et al., 2016). Together, these components contribute to the unique features of the skeletal muscle tissue and the fresh meat, including its strength, flexibility, and elasticity. It has been and still is challenging to recreate those characteristics in an in vitro condition of cultured meat production. One of the main obstacles in this process is the co-culturing of different cell types with distinct properties. In this study, we overcame this limitation of co-culturing different types of cells by utilizing a single source cell to generate various meat components, including muscle, fat and collagen. Precisely, we employed chicken fibroblasts to produce muscle, deposit fat, and synthesize collagen in a well-controlled and adjustable manner within a 3D setting to produce meat with desirable characteristics.

Fibroblasts are the one of the most common cell types in the animal and could serve as the seed cell for cultured meat production due to their unique and versatile features. First, the fibroblast cells are widely available in the bodies of agricultural animals and could be easily isolated and cultured in vitro. Second, many groups have successfully transformed the chicken fibroblasts into immortalized cell lines (Himly et al., 1998; Pasitka et al., 2023). These cell lines can provide an unlimited cellular resource for cultured meat production and eliminate the need for animal or embryo harvest. Third, fibroblasts are capable of adapting to low serum concentration medium or even serum-free medium, which greatly reduce the culturing cost and risk of serum-bound pathogens (Genbacev et al., 2005; Lohr et al., 2009; Pasitka et al., 2023). Last, the fibroblast cells can also undergo transformation to enable high-density propagation in suspension culture (Bürgin et al., 2020; Fluri et al., 2012; Shittu et al., 2016), which is a crucial step towards scaling up to mass-production. The Food and Drug Administration (FDA) has already approved the use of chicken fibroblast cells for cultured meat production and recently, Eat Just Inc. successfully utilized chicken fibroblasts for the commercial production and sale of cultured meat in Singapore and

USA (FDA, 2023). One latest study has also demonstrated the feasibility and consumer acceptance of cultured meat derived solely from native chicken fibroblast cells, indicating a very promising development. However, the resulting meat products do not seem to contain any muscle components (Pasitka et al., 2023). We have previously established an effective strategy for myogenic transdifferentiation, allowing for the production of muscle cells from fibroblast cells of various species in 2D culture (Ren et al., 2022). In the present study, we further enhanced the myogenic transdifferentiation process in 3D, and simultaneously simulated the fat deposition to create cell-based meat that more closely resembles real meat. As a proof-of-concept, we utilized the transgene method to achieve maximum myogenic induction and the final products still retain the foreign transgene fragment in the cells' genome. It is therefore posing a risk of genetic modified food which is not suitable for mass production. In the next step, other non-transgenic means such as non-integrating vectors, chemical reprogramming, modified RNAs, and recombinant transgene removal techniques will be explored to develop transgene-free end products. Another food safety concern in this study is the use of GelMA hydrogel for culture meat production. Due to its excellent biocompatibility and mechanical flexibility, GelMA-based hydrogel has demonstrated significant potential in scalable 3D cell culture for creating artificial tissue ranging in sizes from millimeters to centimeters. It is widely used in 3D cell culture and tissue engineering for regenerative medicine, but less common in food processing and agricultural applications. Due to its special photo-crosslinking properties, biocompatibility and degradability, it allows this material to be shaped into complex tissue structures by 3D printing or modelling. Many researchers have also used GelMA hydrogel as a scaffold for culture meat production (Jeong et al., 2022; Li et al., 2021; Park et al., 2023). Later research will carefully consider hydrogel as well as other types of scaffold biomaterials for cost-effective and food-safety compliant culture meat production (Bomkamp et al., 2022).

Numerous studies have identified the crucial role of fat in the aroma, juiciness, and tenderness of meat. In general, a very low level of intramuscular fat results in dry meat with plain taste, whereas the high intramuscular fat contents can improve the cooking flavor and greatly increase the value of meat products, such as the high marbling beef from Japanese Wagyu cattle (Gotoh et al., 2018; Motoyama et al., 2016). The fat content of fresh meat mainly come from lipids contained in the fat cells. Thus, closely mimicking the intramuscular fat properties in cultured meat would require co-culturing

466 of muscle cells with fat cells. For example, co-culturing pre-adipocytes with myoblasts
467 may increase the intramuscular fat content, tenderness, and taste intensity of cultured
468 meat (Lau et al., 1996; Pandurangan and Kim, 2015; Zagury et al., 2022). However, co-
469 culture of different cell types is technically challenging, since each cell type grows and
470 differentiates in specific optimized medium. When different cell types are cultured in
471 the same medium, these culture conditions may be sub-optimal for one cell type or the
472 other and result in inefficient cellular growth (Pallaoro et al., 2023). Previous studies
473 have underlined the influence adipocytes growing near muscle cells can impair
474 myogenesis (Seo et al., 2019; Takegahara et al., 2014). Simultaneously or sequentially
475 induction of both myogenic and lipogenic differentiation in the same starting seed cells
476 would resolve these co-culture conflicts and the multi-lineage competent chicken
477 fibroblast cells were chosen to explore this double transdifferentiation strategy. As a
478 proof-of-concept, we successfully transformed chicken fibroblast cells into muscle cells
479 and deposited fat into the same cells in 3D hydrogel matrix. Notably, the intramuscular
480 fat content in the cultured meat could be tailored to any specific value within a certain
481 range. From a nutritional point of view, a direct comparison with the traditional chicken
482 meat was performed. The triglyceride content in the cultured meat is comparable to that
483 of chicken meat and more importantly, the amount of fat could be easily manipulated
484 in order to achieve a more attractive nutritional profile.
485
486 In this study, the deposition of fat in the myotubes/myofibers facilitated the storage of
487 significant lipid quantities in transdifferentiated muscle cells, known as
488 intramyocellular lipids. Additionally, we observed Oil Red O staining in the remaining
489 un-transdifferentiated fibroblasts, resembling cells of intramuscular adipocytes
490 (extramyocellular lipids) found within muscle tissue. Hence, current adipogenic
491 induction treatment caused lipogenesis in both the MyoD-transdifferentiated cells and
492 un-transdifferentiated fibroblasts. At present, we don’t know if the fatty acids profile
493 would be different between the two types of origins. The unsaturated fats are
494 conventionally regarded as 'healthier' than saturated fats (Berglund et al., 2007; Hamley,
495 2017). One of the superior assets of cultured meat production is the ability to increase
496 the unsaturated fat levels by adjusting the additive fatty acids, oleic/linoleic acids in this
497 case, in the culture medium. In the future, it requires further comprehensive analysis of
498 the fatty acids profile in the cultured meat to elucidate the fat-associated attributes
499 similar or distinct to real meat.
500

501 The current transcriptome analysis during the cellular transdifferentiation also revealed
502 key regulatory signaling pathways control the formation of cultured meat derived from
503 fibroblasts. Notably, we found several multi-functional pathways such as JAK-STAT,
504 MAPK signaling pathways were significantly enriched in the final cells underwent
505 double myogenic/adipogenic transdifferentiation. These signalings could drive the
506 differentiation process of many different types of cells including muscle and adipose
507 tissues (Bost et al., 2005; Jang and Baik, 2013; Keren et al., 2006; Richard and Stephens,
508 2011), and may be manipulated in current settings to further improve the generation of
509 final cultured meat with tunable fat content.
510
511 In conclusion, we have effectively utilized immortalized chicken fibroblasts in
512 conjunction with classical myogenic/adipogenic transdifferentiation approaches within
513 3D hydrogel to establish a cultured meat model. This model allows for the precise
514 regulation of the synthesis of key components found in conventional meat, including
515 muscle, fat, and ECM. This approach can be readily extrapolated to other species such
516 as pigs and presents promising avenues for the large-scale production of customized
517 and versatile meat products that may cater to varying consumer preferences.
518
519 **Materials and Methods**
520 **Cell preparation and inducible myogenic transdifferentiation**
521 The transdifferentiation cells were constructed as described previously (Ren et al.,
522 2022). Briefly, we cloned the chicken full MyoD coding sequence fused in-frame with
523 3xFlag into a DOX-inducible lentiviral system (Tet-On-MyoD). The wild-type chicken
524 fibroblasts were deal with viral infection and puromycin selection (Invivogen, #ant-pr-
525 1), and finally obtained the transdifferentiation cell lines. In addition, myofibroblasts
526 were isolated from the skin of 10-day-old chicken embryos in the same way as in the
527 previous study (Kosla et al., 2013). Cells were cultured in a 1640 basal medium (Gibco,
528 #C11875500BT) supplemented with 12% fetal bovine serum (FBS) (Gibco, #10270-
529 106) and 1% penicillin-streptomycin (Gibco, #11140050) at 39°C under 5% CO_2
530 atmosphere and were given fresh medium every two days. When grown to
531 approximately 80% confluence, the cells were trypsinized and passaged.
532
533 **Domestication of cells in low concentration serum medium**
534 The chicken fibroblast cells were domesticated with the progressive concentration of
535 serum. In general, cells were cultured with 12% FBS in a 1640 basal medium and when

536 grown to about 80% confluence, the medium was replaced with 6% FBS medium for
537 further cell culture and passage. The medium was then changed to 3% FBS medium for
538 further cell culture and passage depending on the cell status, and so on. Start again and
539 repeat above steps as soon as the cells grow badly or die. We directly changed the cell
540 culture medium from 12% FBS to 2% CS then reduced it to 1% CS when using chicken
541 serum (CS) (Solarbio, #S9080) medium and the cells could adapt to the medium with
542 low concentration of chicken serum after 3-5 passages.
543
544 **Preparation of 3D scaffold and cell culture in 3D matirx**
545 GelMA hydrogels were purchased from Beijing ShangPu for this experiment. Weigh
546 the appropriate amount of GelMA powder into 1640 basal medium, dissolve in a water
547 bath at 70°C for about 30 min, and then filter with 0.22μm sieve. Add 1/8 volume of
548 lithium acylphosphinate salt photoinitiator to the dissolution solution to obtain GelMA
549 hydrogel solution, store at 37°C until usage but no more than 24 h. Fibroblast cells were
550 obtained by trypsin treatment and suspended with GelMA hydrogel solution and gently
551 mixed, followed by treatment of 405nm UV light for 10-20 s to get a 3D hydrogel
552 scaffold. In addition, the hydrogel is secured on a fixation ring for better cell growth
553 and easy movement (Figure S9A and S9B). Place the cell hydrogel complexes in 24-
554 well plate and culture with 1640 medium containing 12%FBS. Transferred to a new
555 well after 12 h, fresh medium was added and changed every 24 h. The cell hydrogel
556 complexes were gently washed three times with PBS buffer and digested by joining
557 collagen II enzyme (Sigma, #10270-106) in incubator at 39°C for 6 min until the cells
558 in the hydrogel package become rounding and shedding. Terminate digest by adding
559 medium and then centrifuged at 1,000 g for 10 min at room temperature (25°C).
560
561 **Cell Counting Kit-8 Assay**
562 Cells cultured in 1% CS and 12% FBS were seeded into 96-well plates with 100 μL of
563 medium per well and incubated for 0 h, 24 h, 48 h and 72 h. 10 μL of the cell Counting
564 Kit-8 Assay (CCK-8) solution (Solarbio, #CA1210, China) was then added to each well
565 and incubated for 2 h. The absorbance values at 450 nm were measured by an EnSpire
566 multifunctional spectrophotometer (Perkin Elmer, USA).
567
568 **EdU assay**
569 2D cells were cultured in 6-well plates, and 1 mL of the growth medium was added to
570 each well with 0.25 μL of 1.25 mg/mL 5-Ethynyl-2'-deoxyuridine (EdU) (Beyotime,

571 #ST067-1g). After 30 min of incubation, cells were fixed by 4% paraformaldehyde
572 (PFA) for 30 min. Cells were stained with a prepared reaction solution consisting of
573 1:100 $CuSO_4$, 1:4 Tris-HCl, 0.017 g/mL ascorbic acid, 1:1000 Alexa Fluor555 dye and
574 pure water. After 30 min, wash it with PBS, and the nuclei were stained with 50 ng/mL
575 DAPI for 10 min. 3D cultures of cells were cultured in 24-well plate dishes by adding
576 1mL of the medium with 0.25μL EdU, incubated for 1 h and then fixed with 4% PFA
577 for 24 h. Staining time extended to 1 h and nuclear staining 20 min. Fluorescence
578 images were collected using fluorescence microscopy.
579
580 **Cell differentiation**
581 For fibroblast induction into myoblasts, 50ng/ml DOX (Sigma, #D3000000) in 1640
582 basal medium containing 12% FBS was added for 3 days and the differentiation
583 medium was replaced when the cells reached 80% fusion. In addition, in 3D culture,
584 cells are proliferated for 7 days before changing the differentiation medium when a
585 dense arrangement of cells can be observed under the microscope.
586 For induction of lipogenic differentiation, the differentiation medium was changed
587 when the fusion rate of cells reached 80% in 2D culture or proliferated for 5 to 7 days
588 in 3D culture. The lipogenesis induction was for 48h with fresh medium changes every
589 24h. For the differentiation experiments, 1640 with 12% FBS was used as a control,
590 and the lipogenic medium was consistent with a 1:100 fatty acid ('F' for short)
591 composition of 1:1 oleic acid (Sigma, #O3008, 2 mol oleic acid/mole albumin) and
592 linoleic acids (Sigma, #L9530, 2 mol linoleic acid/mole albumin; 100 mg/mL albumin),
593 and insulin ('I' for short) (Sigma, #I0516) concentration of 60 μg/mL.
594
595 **Immunofluorescence staining**
596 Similar as our previous steps for immunofluorescence staining of cells in 2D culture
597 (Luo et al., 2022), cells were fixed in 4% PFA for 30 min and washed three times with
598 PBS buffer at room temperature, then permeabilizing with 0.5% Triton X-100 on PBS
599 for 10 min and blocking with 10% goat serum at 0.5% TritonX-100 for 1 h. Primary
600 antibodies were diluted with 10% goat serum in 0.5% Triton X-100 at 4°C for 12 h. The
601 primary antibody for MHC (DSHB, #AB2147781) and the primary antibody for
602 Desmin (Sigma, #D8281) and laminin (Sigma, #F1804) were added at a dilution of
603 1:500 and the primary antibody for Vimentin (DSHB, #AB528504) at a dilution of
604 1:200. Followed by incubation with Alexa secondary antibody (Invitrogen, #A-21202,
605 #A-21206 and #A-31570) at a 1:500 dilution for 2 h at room temperature. Antibody for

606 α-SMA (Sigma, C6198) was added at a dilution of 1:500 and incubated with 10% goat
607 serum in 0.5% Triton X-100 at room temperature for 2h. Nuclear staining was
608 performed with 50 ng/mL DAPI (Sigma, #D8417) for 10 min. Cells in the 3D culture
609 were fixed for 48 h, the total time of permeabilizing and the blocking was no more than
610 24 h, and the incubation time of the primary antibody was extended to 24 h, the
611 secondary antibody was 4 h and the nuclear staining 20 min. For MHC detection,
612 fluorescence images were collected using fluorescence microscopy and the
613 $MHC^{+}DAPI^{+}/DAPI^{+}$ differentiation index was calculated from three or more images
614 using confocal microscopy (Zeiss LSM 800).
615
616 **Oil Red O Staining**
617 For Oil Red O staining, cells were fixed with 4% PFA for 30 min or 24 h respectively
618 in 2D and 3D culture. After washing thrice with PBS at room temperature, the cells
619 were soaked in 60% isopropanol for better coloration of Oil Red and then washed for 5
620 min or 10 min respectively in 2D and 3D culture. The cells were stained with Oil Red
621 O (Sigma, #O0625) for 30 min or 60 min respectively in 2D and 3D. Cells were washed
622 with 60% isopropanol for 30 s or 1 min respectively in 2D and 3D to remove surface
623 staining. Then, cells were washed with distilled water for three times and the stained
624 lipid droplets were visualized using a microscope.
625
626 **mRNA extraction and real-time quantitative PCR (qPCR) and library**
627 **construction**
628 Cells were lysed in Trizol (Simgen, #5301100) and RNA was extracted following
629 manufacture's recommendations. RNA concentration was measured on NanoDrop2000
630 (Thermo Scientific, USA). 1 μg of RNA was reverse transcribed using PrimeScriptTM
631 RT reagent Kit (Takara, #RR047A). Real-time quantitative PCR was performed using
632 SYBR Green Mix (Abclonal, #RK21203) following manufacturer's instructions.
633 Expression was normalized to GAPDH using delta-delta-CT method. For comparisons
634 of the expression, we used a one-tailed Student's t-test. The error bars indicate the SEM.
635 The RT-qPCR primers are described in Table S1. The RNA-Seq library-preparation
636 protocol was based on the NEBNext Ultra™ RNA Library Prep Kit for Illumina (NEB,
637 #E7530L). Insert size was assessed using the Agilent Bioanalyzer 2100 system and
638 qualified insert size was accurate quantification using StepOnePlus™ Real-Time PCR
639 System (Library valid concentration＞10nM) and then paired-end sequencing using an
640 Illumina platform. RNA-Seq was performed on triplicates for each sample.

641

642 **RNA-Seq data analysis**

643 The RNA-Seq raw data were firstly trimmed adapters by trim_galore software (Bolger
644 et al., 2014) and then the clean data of RNA-Seq was mapped to chicken genome
645 (Ensembl, GRCg7b) using hisat2 (Kim et al., 2019) with default parameters. Because
646 of using paired-end reads, the concordant unique mapping reads/pairs were kept based
647 on the mapping flags. The duplications were removed based on the coordinates of the
648 reads/pairs. The de-duplication unique mapping reads/pairs were used for further
649 analysis in this study. Read counts for each sample were computed with the
650 featureCounts (Liao et al., 2014) software and the RefSeq gene annotation for chicken
651 genome assembly is GRCg7b. The transcript per million (TPM) were normalized using
652 reads counts. Differential expressed genes (DEGs) of RNA-Seq data were analyzed
653 using DESeq2 called by $q<0.01$ and fold change >2 thresholds. The chicken genes were
654 transformed to homologue human genes using ensemble bioMart database and the gene
655 ontology in this study was conducted in Metascape and the enriched top pathways were
656 shown. All plots were generated by R (v4.0.3).

657

658 **Measurement of total collagen content in cultured meat**

659 Total collagen content was determined by the concentration of hydroxyproline. The
660 medium was replaced with fresh medium in the incubator for 2 h before the assay,
661 washed three times with PBS. According to the instructions of the Hydroxyproline
662 Assay Kit (Jiancheng, #A030-1-1, China), one volume of saline was added in dried
663 cultured meat at a 1:1 ratio of weight and volume. After mechanical homogenization in
664 ice-water bath, the digestion solution was incubated at 37°C in a water bath for 4 h.
665 Hydroxyproline content was measured by the absorbance at 550 nm using an EnSpire
666 multifunctional spectrophotometer (Perkin Elmer, USA). For each measurement of
667 cultured meat, the hydroxyproline content of the corresponding blank cell-free hydrogel
668 was substracted. The amount of collagen was calculated from the hydroxyproline
669 concentration with a conversion factor of 7.25 in μg/mg wet tissue (Vasanthi et al., 2007;
670 Zheng et al., 2021).

671

672 **Measurement of triglyceride content in cultured meat**

673 The triglyceride content in cultured meat was measured using the kit (Solarbio,
674 #BC0620, China). Before the assay, the culture system is washed three times with PBS
675 and uniformly added to the same medium containing 12% FBS in the incubator for 2 h,

after which it is removed and washed three more times with PBS, the cultured meat is taken out and churned, and the precipitate is obtained by centrifugation, which should be well air-dried. The precipitate was weighed and tirzol was added to lyse well for 2 h. A mixture of n-heptane and isopropanol in a ratio of 1:1 was then added and shaken and mixed. Then added potassium hydroxide and full shaken to produce glycerol and fatty acids, then the other reagents were added in sequence according to the instructions. The final triglyceride content was measured the specific light intensity at 420 nm, as described previously.

Emission scanning electron microscope

The cell hydrogels were washed three times with PBS and then fixed in 4% PFA for 1 h. Samples were randomly clamped into spiking trays, rapidly frozen in liquid nitrogen and then images were randomly collected using the emission scanning electron microscope (HITACHI SU8010, Japan).

Statistical analyses

Statistical analyses were performed using the Graph-Pad Prism software. For normally distributed data sets with equal variances, a two-sample t-test was used. The significance of differences was provided in figure legends.

Acknowledgements

This work was supported by National Natural Science Foundation of China (31771617), Taishan Scholar Program, Scientific Research Innovation Team of Young Scholar of Shandong.

References

Addison, W.N., Fu, M.M., Yang, H.X., Lin, Z., Nagano, K., Gori, F., and Baron, R. (2014). Direct transcriptional repression of Zfp423 by Zfp521 mediates a bone morphogenic protein-dependent osteoblast versus adipocyte lineage commitment switch. Mol Cell Biol *34*, 3076-3085.

Bakkar, N., and Guttridge, D.C. (2010). NF-kappaB signaling: a tale of two pathways in skeletal myogenesis. Physiological reviews *90*, 495-511.

Batista, M.L., Jr., Peres, S.B., McDonald, M.E., Alcantara, P.S., Olivan, M., Otoch, J.P., Farmer, S.R., and Seelaender, M. (2012). Adipose tissue inflammation and cancer cachexia: possible role of nuclear transcription factors. Cytokine *57*, 9-16.

Ben-Arye, T., and Levenberg, S. (2019). Tissue Engineering for Clean Meat Production. Frontiers in Sustainable Food Systems *3*.

Berglund, L., Lefevre, M., Ginsberg, H.N., Kris-Etherton, P.M., Elmer, P.J., Stewart, P.W., Ershow, A., Pearson, T.A., Dennis, B.H., Roheim, P.S.*, et al.* (2007). Comparison of monounsaturated fat with carbohydrates as a replacement for saturated fat in subjects with a high metabolic risk profile: studies in the fasting and postprandial states. Am J Clin Nutr *86*, 1611-1620.

Bolger, A.M., Lohse, M., and Usadel, B. (2014). Trimmomatic: a flexible trimmer for Illumina sequence data. Bioinformatics (Oxford, England) *30*, 2114-2120.

Bost, F., Aouadi, M., Caron, L., and Binétruy, B. (2005). The role of MAPKs in adipocyte differentiation and obesity. Biochimie *87*, 51-56.

Bürgin, T., Coronel, J., Hagens, G., Keebler, M.V., Genzel, Y., Reichl, U., and Anderlei, T. (2020). Orbitally Shaken Single-Use Bioreactor for Animal Cell Cultivation: Fed-Batch and Perfusion Mode. Methods Mol Biol *2095*, 105-123.

Cao, Y., Kumar, R.M., Penn, B.H., Berkes, C.A., Kooperberg, C., Boyer, L.A., Young, R.A., and Tapscott, S.J. (2006). Global and gene-specific analyses show distinct roles for Myod and Myog at a common set of promoters. Embo J *25*, 502-511.

Chriki, S., and Hocquette, J.F. (2020). The Myth of Cultured Meat: A Review. Frontiers in Nutrition *7*.

Fluri, D.A., Tonge, P.D., Song, H., Baptista, R.P., Shakiba, N., Shukla, S., Clarke, G., Nagy, A., and Zandstra, P.W. (2012). Derivation, expansion and differentiation of induced pluripotent stem cells in continuous suspension cultures. Nat Methods *9*, 509-516.

Franco-Barraza, J., Beacham, D.A., Amatangelo, M.D., and Cukierman, E. (2016). Preparation of Extracellular Matrices Produced by Cultured and Primary Fibroblasts. Curr Protoc Cell Biol *71*, 10.19.11-10.19.34.

Frank, D., Ball, A., Hughes, J., Krishnamurthy, R., Piyasiri, U., Stark, J., Watkins, P., and Warner, R. (2016). Sensory and Flavor Chemistry Characteristics of Australian Beef: Influence of Intramuscular Fat, Feed, and Breed. J Agric Food Chem *64*, 4299-4311.

French, M.M., Rose, S., Canseco, J., and Athanasiou, K.A. (2004). Chondrogenic differentiation of adult dermal fibroblasts. Ann Biomed Eng *32*, 50-56.

Genbacev, O., Krtolica, A., Zdravkovic, T., Brunette, E., Powell, S., Nath, A., Caceres, E., McMaster, M., McDonagh, S., Li, Y.*, et al.* (2005). Serum-free derivation of human embryonic stem cell lines on human placental fibroblast feeders. Fertil Steril *83*, 1517-1529.

Gotoh, T., Nishimura, T., Kuchida, K., and Mannen, H. (2018). The Japanese Wagyu beef industry: current situation and future prospects - A review. Asian-Australas J Anim Sci *31*, 933-950.

Hamley, S. (2017). The effect of replacing saturated fat with mostly n-6 polyunsaturated fat on coronary heart disease: a meta-analysis of randomised controlled trials. Nutr J *16*, 30.

745 Hausman, G.J. (2012). MEAT SCIENCE AND MUSCLE BIOLOGY SYMPOSIUM: The influence of
746 extracellular matrix on intramuscular and extramuscular adipogenesis. J Anim Sci *90*, 942-949.
747 Hecker, L., Jagirdar, R., Jin, T., and Thannickal, V.J. (2011). Reversible differentiation of myofibroblasts
748 by MyoD. Exp Cell Res *317*, 1914-1921.
749 Himly, M., Foster, D.N., Bottoli, I., Iacovoni, J.S., and Vogt, P.K. (1998). The DF-1 chicken fibroblast
750 cell line: Transformation induced by diverse oncogenes and cell death resulting from infection by avian
751 leukosis viruses. Virology *248*, 295-304.
752 Hinz, B., Phan, S.H., Thannickal, V.J., Galli, A., Bochaton-Piallat, M.L., and Gabbiani, G. (2007). The
753 myofibroblast: one function, multiple origins. Am J Pathol *170*, 1807-1816.
754 Jang, Y.N., and Baik, E.J. (2013). JAK-STAT pathway and myogenic differentiation. Jak-stat *2*, e23282.
755 Jeong, D., Seo, J.W., Lee, H.G., Jung, W.K., Park, Y.H., and Bae, H. (2022). Efficient
756 Myogenic/Adipogenic Transdifferentiation of Bovine Fibroblasts in a 3D Bioprinting System for Steak-
757 Type Cultured Meat Production. Adv Sci *9*.
758 Keren, A., Tamir, Y., and Bengal, E. (2006). The p38 MAPK signaling pathway: a major regulator of
759 skeletal muscle development. Molecular and cellular endocrinology *252*, 224-230.
760 Kim, D., Paggi, J.M., Park, C., Bennett, C., and Salzberg, S.L. (2019). Graph-based genome alignment
761 and genotyping with HISAT2 and HISAT-genotype. Nature biotechnology *37*, 907-915.
762 Kim, D.H., Lee, J., Suh, Y., Cressman, M., and Lee, K. (2021). Research Note: Adipogenic differentiation
763 of embryonic fibroblasts of chicken, turkey, duck, and quail in vitro by medium containing chicken serum
764 alone. Poultry Sci *100*.
765 Kim, D.H., Lee, J., Suh, Y., Cressman, M., Lee, S.S., and Lee, K. (2020). Adipogenic and Myogenic
766 Potentials of Chicken Embryonic Fibroblasts in vitro: Combination of Fatty Acids and Insulin Induces
767 Adipogenesis. Lipids *55*, 163-171.
768 Kosla, J., Dvorak, M., and Cermak, V. (2013). Molecular analysis of the TGF-beta controlled gene
769 expression program in chicken embryo dermal myofibroblasts. Gene *513*, 90-100.
770 Lau, D.C.W., Shillabeer, G., Li, Z.H., Wong, K.L., Varzaneh, F.E., and Tough, S.C. (1996). Paracrine
771 interactions in adipose tissue development and growth. Int J Obesity *20*, S16-S25.
772 Lee, J., Kim, D.H., Suh, Y., and Lee, K. (2021). Research Note: Potential usage of DF-1 cell line as a
773 new cell model for avian adipogenesis. Poultry Sci *100*.
774 Liao, Y., Smyth, G.K., and Shi, W. (2014). featureCounts: an efficient general purpose program for
775 assigning sequence reads to genomic features. Bioinformatics (Oxford, England) *30*, 923-930.
776 Lohr, V., Rath, A., Genzel, Y., Jordan, I., Sandig, V., and Reichl, U. (2009). New avian suspension cell
777 lines provide production of influenza virus and MVA in serum-free media: studies on growth, metabolism
778 and virus propagation. Vaccine *27*, 4975-4982.
779 Longo, M., Raciti, G.A., Zatterale, F., Parrillo, L., Desiderio, A., Spinelli, R., Hammarstedt, A.,
780 Hedjazifar, S., Hoffmann, J.M., Nigro, C.*, et al.* (2018). Epigenetic modifications of the Zfp/ZNF423
781 gene control murine adipogenic commitment and are dysregulated in human hypertrophic obesity.
782 Diabetologia *61*, 369-380.
783 Luo, W., Xu, Y., Liu, R., Liao, Y., Wang, S., Zhang, H., Li, X., and Wang, H. (2022). Retinoic acid and
784 RARγ maintain satellite cell quiescence through regulation of translation initiation. Cell Death Dis *13*,
785 838.
786 Mattick, C.S., Landis, A.E., and Allenby, B.R. (2015). A case for systemic environmental analysis of
787 cultured meat. Journal of Integrative Agriculture *14*, 249-254.
788 Motoyama, M., Sasaki, K., and Watanabe, A. (2016). Wagyu and the factors contributing to its beef

789 quality: A Japanese industry overview. Meat Sci *120*, 10-18.
790 Nakashima, K., Yamazaki, M., and Abe, H. (2005). Effects of serum deprivation on expression of
791 proteolytic-related genes in chick myotube cultures. Biosci Biotechnol Biochem *69*, 623-627.
792 Pallaoro, M., Modina, S.C., Fiorati, A., Altomare, L., Mirra, G., Scocco, P., and Di Giancamillo, A.
793 (2023). Towards a More Realistic In Vitro Meat: The Cross Talk between Adipose and Muscle Cells. Int
794 J Mol Sci *24*.
795 Pandurangan, M., and Kim, D.H. (2015). A novel approach for in vitro meat production. Appl Microbiol
796 Biot *99*, 5391-5395.
797 Pasitka, L., Cohen, M., Ehrlich, A., Gildor, B., Reuveni, E., Ayyash, M., Wissotsky, G., Herscovici, A.,
798 Kaminker, R., Niv, A.*, et al.* (2023). Spontaneous immortalization of chicken fibroblasts generates stable,
799 high-yield cell lines for serum-free production of cultured meat (Dec, 10.1038/s43016-022-00658-w,
800 2022). Nature Food *4*, 124-124.
801 Paulin, D., and Li, Z. (2004). Desmin: a major intermediate filament protein essential for the structural
802 integrity and function of muscle. Exp Cell Res *301*, 1-7.
803 Pepelanova, I., Kruppa, K., Scheper, T., and Lavrentieva, A. (2018). Gelatin-methacryloyl (GelMA)
804 hydrogels with defined degree of functionalization as a versatile toolkit for 3D cell culture and extrusion
805 bioprinting. Bioengineering *5*, 55.
806 Relaix, F., Demignon, J., Laclef, C., Pujol, J., Santolini, M., Niro, C., Lagha, M., Rocancourt, D.,
807 Buckingham, M., and Maire, P. (2013). Six homeoproteins directly activate Myod expression in the gene
808 regulatory networks that control early myogenesis. PLoS Genet *9*, e1003425.
809 Ren, R.M., Fan, Y., Peng, Z.L., Wang, S., Jiang, Y.Q., Fu, L.L., Cao, J.H., Zhao, S.H., and Wang, H.
810 (2022). Characterization and perturbation of CTCF-mediated chromatin interactions for enhancing
811 myogenic transdifferentiation. Cell Reports *40*.
812 Richard, A.J., and Stephens, J.M. (2011). Emerging roles of JAK-STAT signaling pathways in adipocytes.
813 Trends in endocrinology and metabolism: TEM *22*, 325-332.
814 Seo, K., Suzuki, T., Kobayashi, K., and Nishimura, T. (2019). Adipocytes suppress differentiation of
815 muscle cells in a co-culture system. Anim Sci J *90*, 423-434.
816 Shittu, I., Zhu, Z., Lu, Y., Hutcheson, J.M., Stice, S.L., West, F.D., Donadeu, M., Dungu, B., Fadly, A.M.,
817 Zavala, G.*, et al.* (2016). Development, characterization and optimization of a new suspension chicken-
818 induced pluripotent cell line for the production of Newcastle disease vaccine. Biologicals *44*, 24-32.
819 Takase, S., Leo, M.A., Nouchi, T., and Lieber, C.S. (1988). Desmin distinguishes cultured fat-storing
820 cells from myofibroblasts, smooth muscle cells and fibroblasts in the rat. J Hepatol *6*, 267-276.
821 Takegahara, Y., Yamanouchi, K., Nakamura, K., Nakano, S., and Nishihara, M. (2014). Myotube
822 formation is affected by adipogenic lineage cells in a cell-to-cell contact-independent manner. Exp Cell
823 Res *324*, 105-114.
824 Tarbit, E., Singh, I., Peart, J.N., and Rose'Meyer, R.B. (2019). Biomarkers for the identification of cardiac
825 fibroblast and myofibroblast cells. Heart Fail Rev *24*, 1-15.
826 van Rooij, E., Quiat, D., Johnson, B.A., Sutherland, L.B., Qi, X., Richardson, J.A., Kelm, R.J., Jr., and
827 Olson, E.N. (2009). A family of microRNAs encoded by myosin genes governs myosin expression and
828 muscle performance. Dev Cell *17*, 662-673.
829 Vasanthi, C., Venkataramanujam, V., and Dushyanthan, K. (2007). Effect of cooking temperature and
830 time on the physico-chemical, histological and sensory properties of female carabeef (buffalo) meat.
831 Meat Sci *76*, 274-280.
832 Vaughan, M.B., Howard, E.W., and Tomasek, J.J. (2000). Transforming growth factor-beta1 promotes

the morphological and functional differentiation of the myofibroblast. Exp Cell Res *257*, 180-189.

Vincent, C.K., Gualberto, A., Patel, C.V., and Walsh, K. (1993). Different regulatory sequences control creatine kinase-M gene expression in directly injected skeletal and cardiac muscle. Mol Cell Biol *13*, 1264-1272.

Warkman, A.S., Whitman, S.A., Miller, M.K., Garriock, R.J., Schwach, C.M., Gregorio, C.C., and Krieg, P.A. (2012). Developmental expression and cardiac transcriptional regulation of Myh7b, a third myosin heavy chain in the vertebrate heart. Cytoskeleton (Hoboken) *69*, 324-335.

Weintraub, H., Tapscott, S.J., Davis, R.L., Thayer, M.J., Adam, M.A., Lassar, A.B., and Miller, A.D. (1989). Activation of muscle-specific genes in pigment, nerve, fat, liver, and fibroblast cell lines by forced expression of MyoD. Proc Natl Acad Sci U S A *86*, 5434-5438.

Yin, J., Jin, X., Beck, S., Kang, D.H., Hong, Z., Li, Z., Jin, Y., Zhang, Q., Choi, Y.J., Kim, S.C.*, et al.* (2010). In vitro myogenic and adipogenic differentiation model of genetically engineered bovine embryonic fibroblast cell lines. Biotechnol Lett *32*, 195-202.

Zagury, Y., Ianovici, I., Landau, S., Lavon, N., and Levenberg, S. (2022). Engineered marble-like bovine fat tissue for cultured meat. Commun Biol *5*, 927.

Zheng, Y.Y., Zhu, H.Z., Wu, Z.Y., Song, W.J., Tang, C.B., Li, C.B., Ding, S.J., and Zhou, G.H. (2021). Evaluation of the effect of smooth muscle cells on the quality of cultured meat in a model for cultured meat. Food Res Int *150*, 110786.

852 **Figures and legends**

853

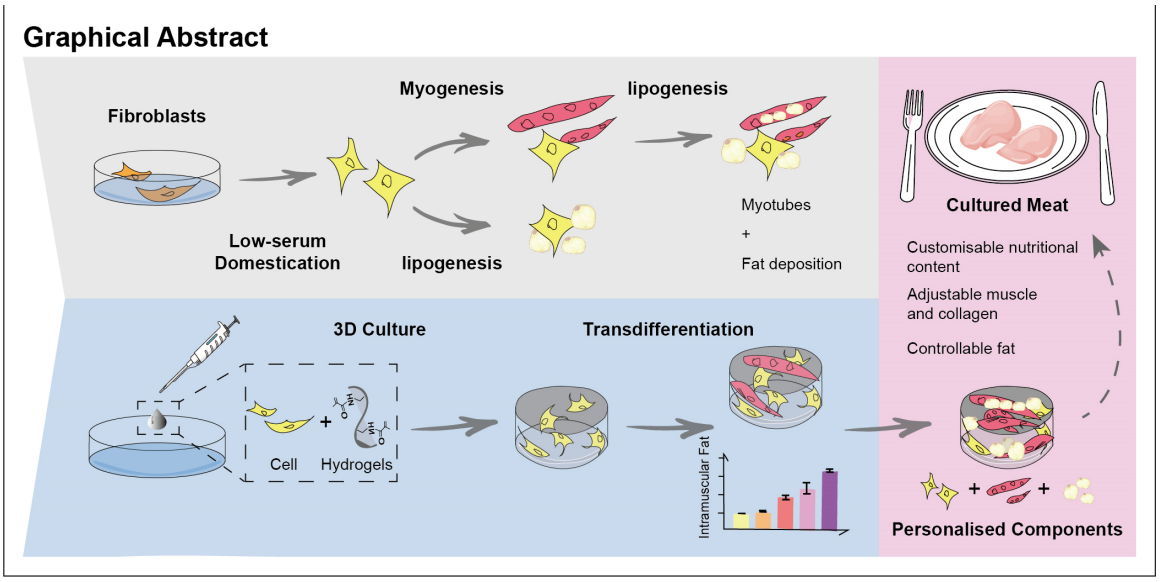

854

855 **Graphical abstract.**

856

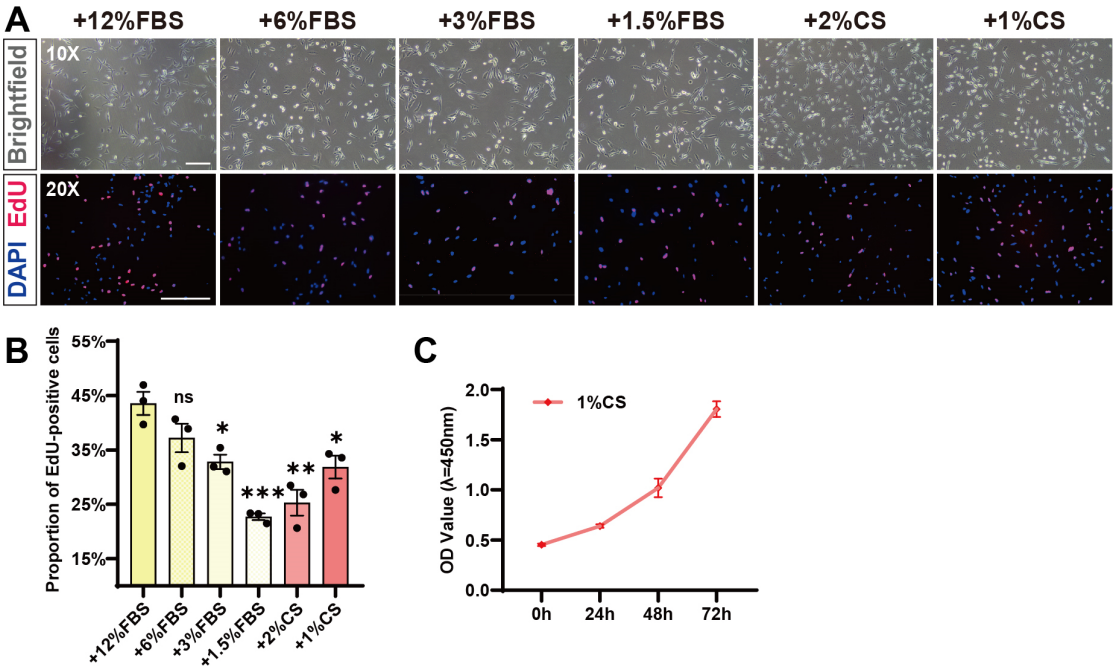

Figure 1. Chicken fibroblasts proliferate stably in low-serum conditions. (A) Cellular morphology and EdU staining of chicken fibroblasts under different low-serum conditions. FBS: Fetal bovine serum. CS: Chicken serum. Scale bar, 200 μm. (B) Quantification of the proportion of EdU-positive cells in Figure A. Error bars indicate s.e.m. n = 3. *P < 0.05, **P < 0.01, ***P < 0.001. (C) The CCK-8 cell proliferation assay showed the proliferation of chicken fibroblasts in 1% chicken serum. Error bars indicate s.e.m, n = 3.

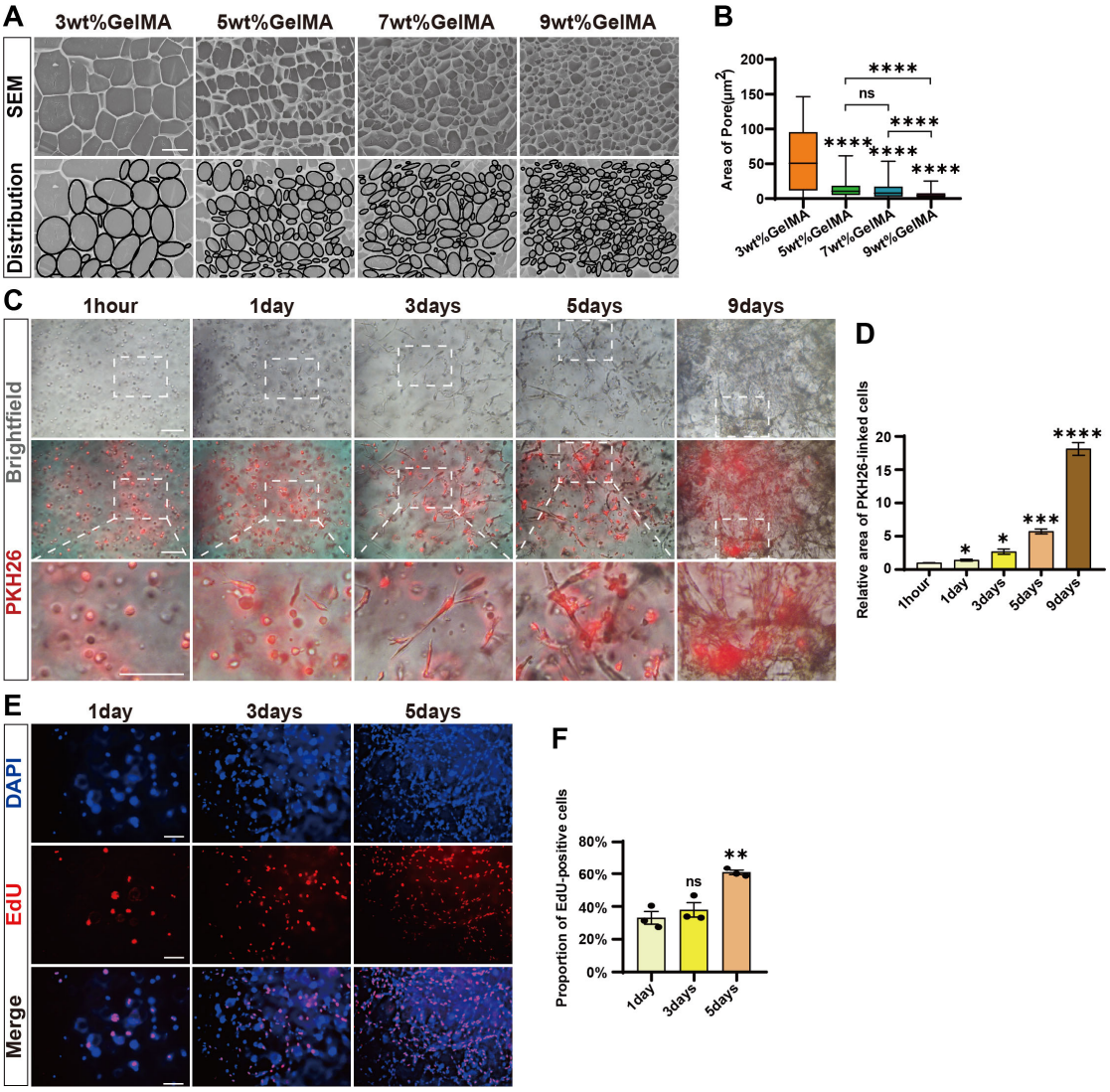

Figure 2. 3D culture of chicken fibroblasts in GelMA hydrogels. (A) Microscopic images of GelMA hydrogels at different concentrations (3%wt, 5%wt, 7%wt and 9%wt) taken by scanning electron microscopy and their corresponding simplified maps of pore distributions. Scale bar, 10 μm. (B) Quantification of pore area in image A. Error bars indicate s.e.m, n = 3. ****P < 0.0001. (C) Brightfield and red fluorescent images of cells in 3D culture after PKH26 staining at different times (1hour, 1day, 3days, 5days and 9days). Scale bar, 100 μm. (D) Relative area of PKH26-linked cells in Figure C. Error bars indicate s.e.m, n = 3. *P < 0.05, ***P < 0.001, ****P < 0.0001. (E) Representative EdU staining shows the proliferation of cells in 3D culture on 1day, 3days and 5 days after cell implantation in hydrogel. Scale bar, 100 μm. (F) Quantification of the proportion of EdU-positive cells in Figure E. Error bars indicate s.e.m, n = 3. **P < 0.01.

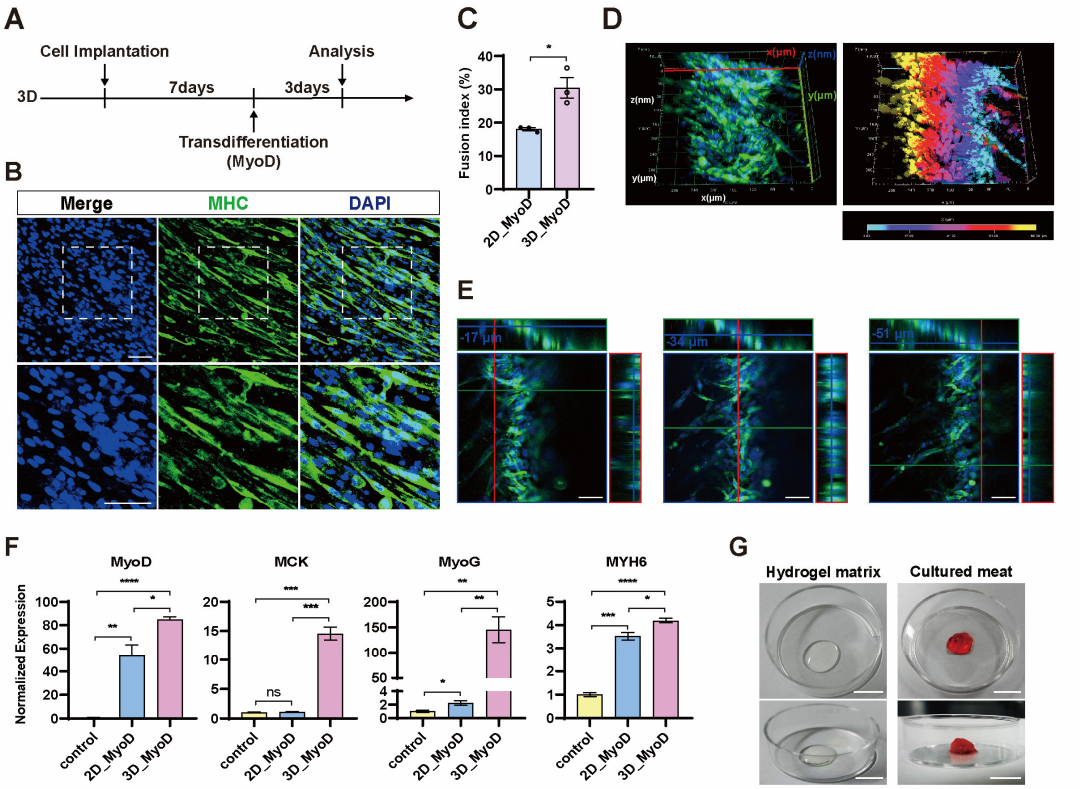

Figure 3. Transdifferentiation of chicken fibroblasts into muscle cells in 3D. (A) Experimental design for fibroblast myogenic transdifferentiation in 3D culture. (B) Representative images of MHC staining showed the myogenic ability of chicken fibroblasts in 3D culture. Scale bar, 50 μm. (C) Comparison of the mean myogenic fusion index between 2D and 3D. Error bars indicate s.e.m, n = 3. *P < 0.05. (D) Three-dimensional images of MHC staining of cells cultured in 3D. The right panel is its depth-coded image which indicate different depths from the deepest (cyan) to the surface (yellow). (E) Orthogonal projections of three sets of MHC staining of cells in 3D culture at different depths. Scale bar, 50 μm. (F) Expression of skeletal muscle-related genes was determined by RT-qPCR in 2D and 3D cells upon myogenic transdifferentiation and control 3D cells without stimulation. Please note that the myogenic transdifferentiation driven by MyoD stimulate the expression of classical myogenic factors. Error bars indicate s.e.m, n = 3. *P < 0.05, **P < 0.01, ***P < 0.001, ****P < 0.0001. (G) Macroscopic morphology of the empty hydrogel matrix (left) and cultured meat (right). The cultured meat is the product obtained after 3D cell culture and induction of myogenesis/lipogenesis. Scale bar, 1 cm.

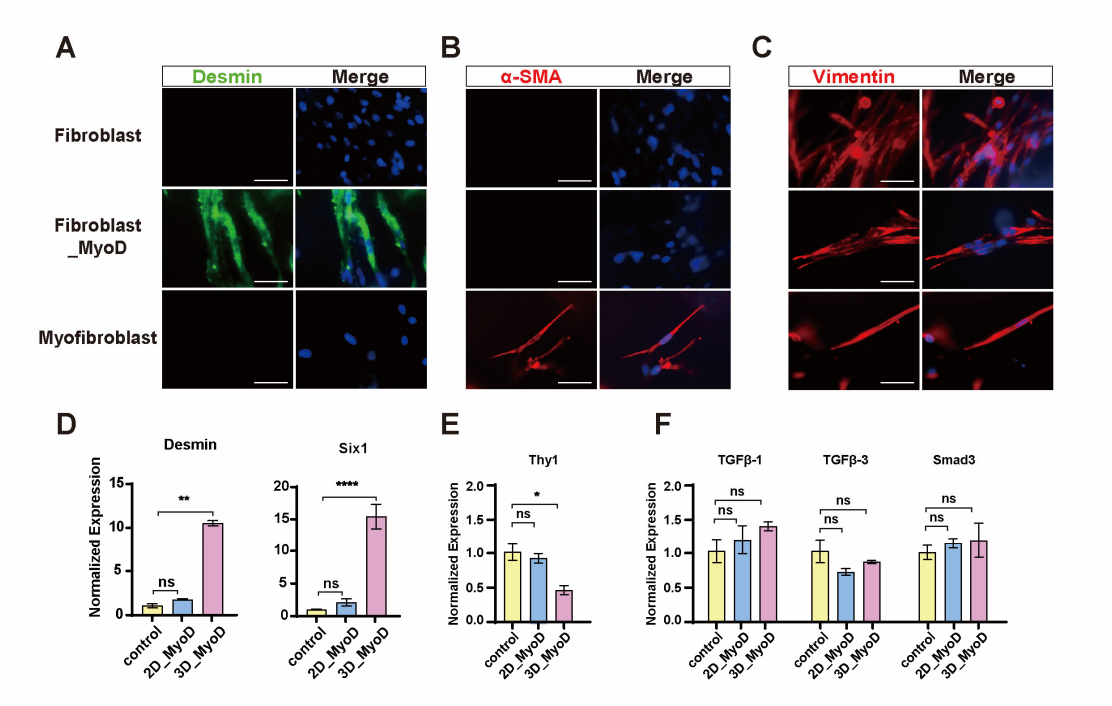

Figure 4. Myogenic transdifferentiation of fibroblasts do not produce myofibroblasts. (A) Immunofluorescence staining of 3D cultured cells showed that the skeletal muscle marker desmin was expressed only in the transdifferentiated cells but not in fibroblasts or myofibroblasts. Scale bar, 50 μm. (B) Immunofluorescence staining of 3D cultured cells showed that the myofibroblast marker α-SMA was expressed only in the myofibroblasts but not in fibroblasts or transdifferentiated cells. Scale bar, 50 μm. (C) Immunofluorescence staining of 3D cultured cells showed that the fibroblast marker vimentin was abundantly expressed in fibroblasts and myofibroblasts but greatly reduced in transdifferentiated cells. Scale bar, 50 μm. (D) RT-qPCR showed that the myogenic genes Desmin and Six1 were significantly increased upon myogenic transdifferentiation. (E) RT-qPCR showed the fibroblast marker gene Thy-1 was significantly reduced upon myogenic transdifferentiation. (F) The myofibroblast marker genes TGFβ-1, TGFβ-3 and Smad3 remain unchanged during myogenic transdifferentiation. Error bars indicate s.e.m, n = 4. *P < 0.05, **P < 0.01, ***P < 0.001, ****P < 0.0001. ns: not significant.

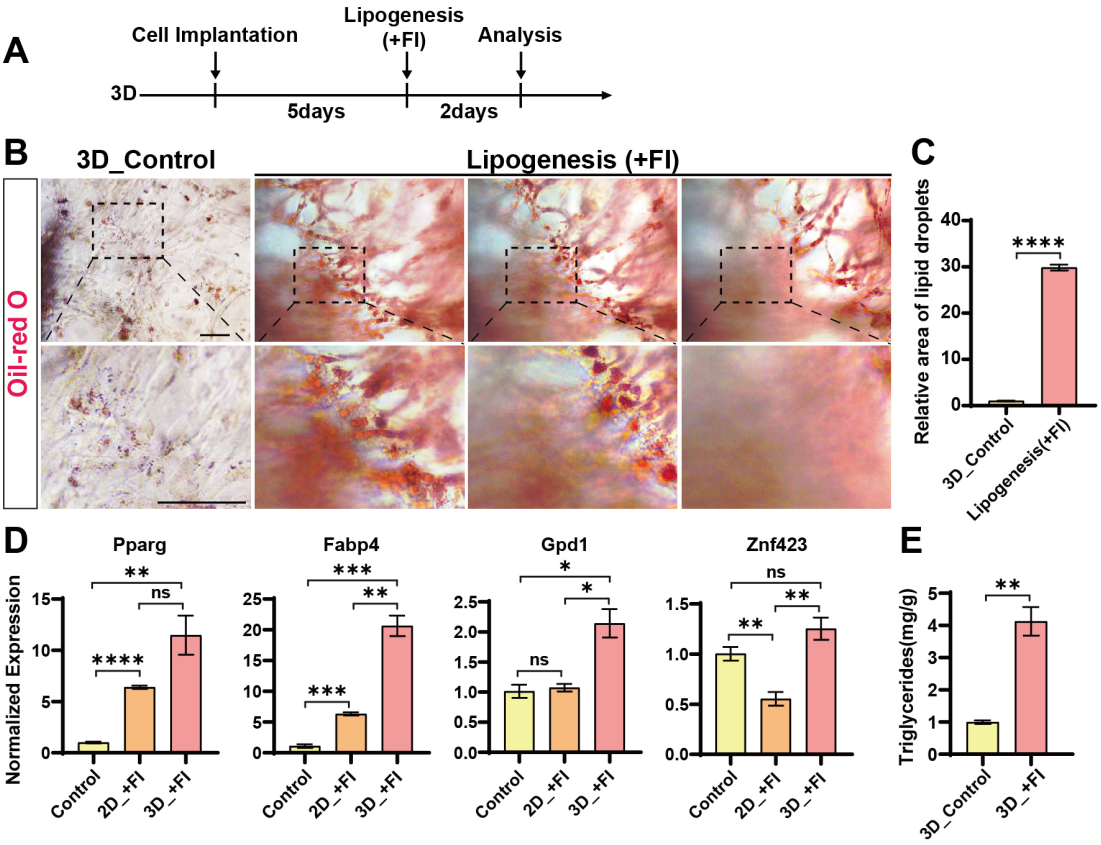

Figure 5. Stimulate the fat deposition in chicken fibroblasts in 3D. (A) Experimental design for fibroblast lipogenesis in 3D culture ('F' is for fatty acids and 'I' is for insulin). (B) Representative images showing the Oil-red O staining of lipid content accumulated in cells at different focal planes at the same position. The control group was normal medium without lipogenesis. Scale bar, 100 μm. (C) Relative area of lipid droplets in figure B. Error bars indicate s.e.m, n = 3. ****P < 0.0001. (D) Expression of lipid synthesis related genes determined by RT-qPCR in 2D and 3D cells upon lipogenic induction and control 3D cells without stimulation. Error bars indicate s.e.m, n = 3. *P < 0.05, **P < 0.01, ***P < 0.001, ****P < 0.0001. (E) Triglyceride content in the cultured meat upon different lipogenic inductions and control 3D cells without stimulation. Error bars indicate s.e.m, n = 3. *P < 0.05, **P < 0.01, ***P < 0.001.

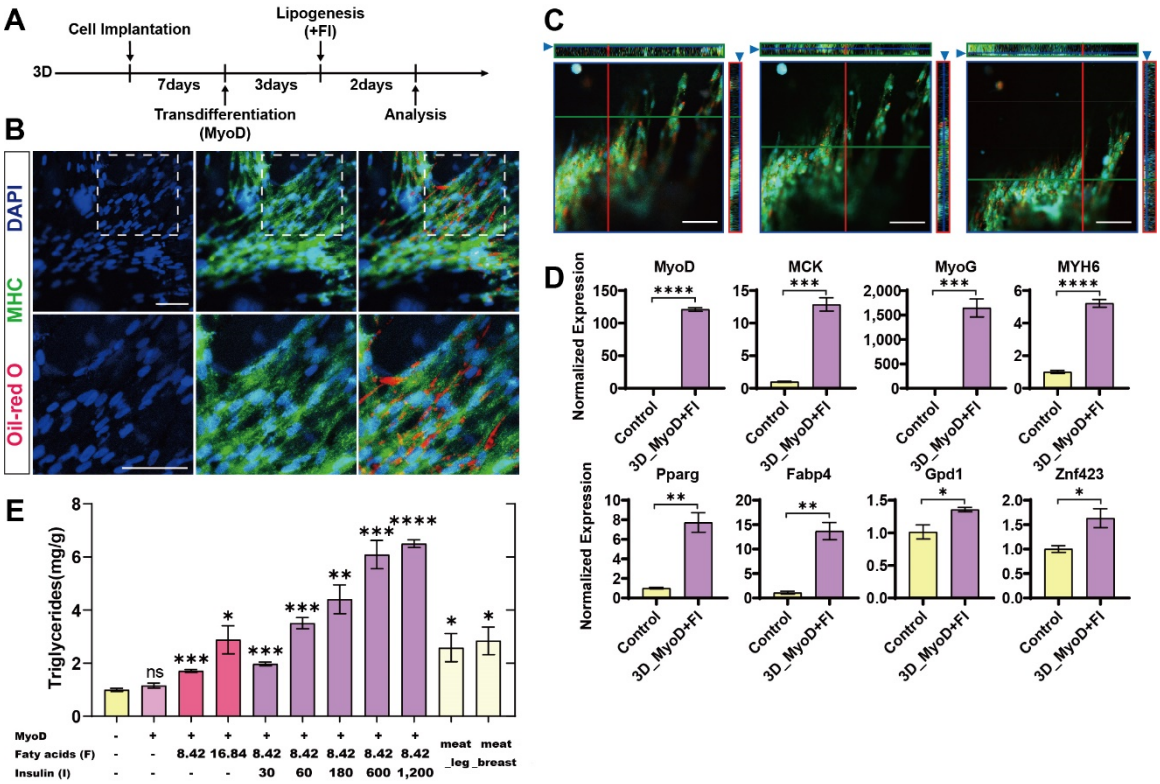

Figure 6. Controlled fat deposition in the transdifferentiated muscle cells in 3D hydrogel. (A) Experimental design for fibroblast myogenic/lipogenic differentiation in 3D culture. (B) Representative images of MHC and Oil Red O staining of cells upon myogenesis/lipogenesis in 3D culture. Scale bar, 50 µm. (C) Orthogonal projections of three sets of MHC and Oil Red O staining of cells in 3D culture at different depths. Scale bar, 50 µm. (D) Expression of muscle-related genes (top) and lipid-related genes (bottom) in the cells with myogenesis/lipogenesis induction and control 3D cells without any stimulation were determined by RT-qPCR. (E) Triglyceride content of cultured meat under different conditions and real meat. “Meat_leg” and “Meat_breast” are taken from the leg and breast muscles of adult chickens. Error bars indicate s.e.m, n = 3. *P < 0.05, **P < 0.01, ***P < 0.001, ****P < 0.0001.

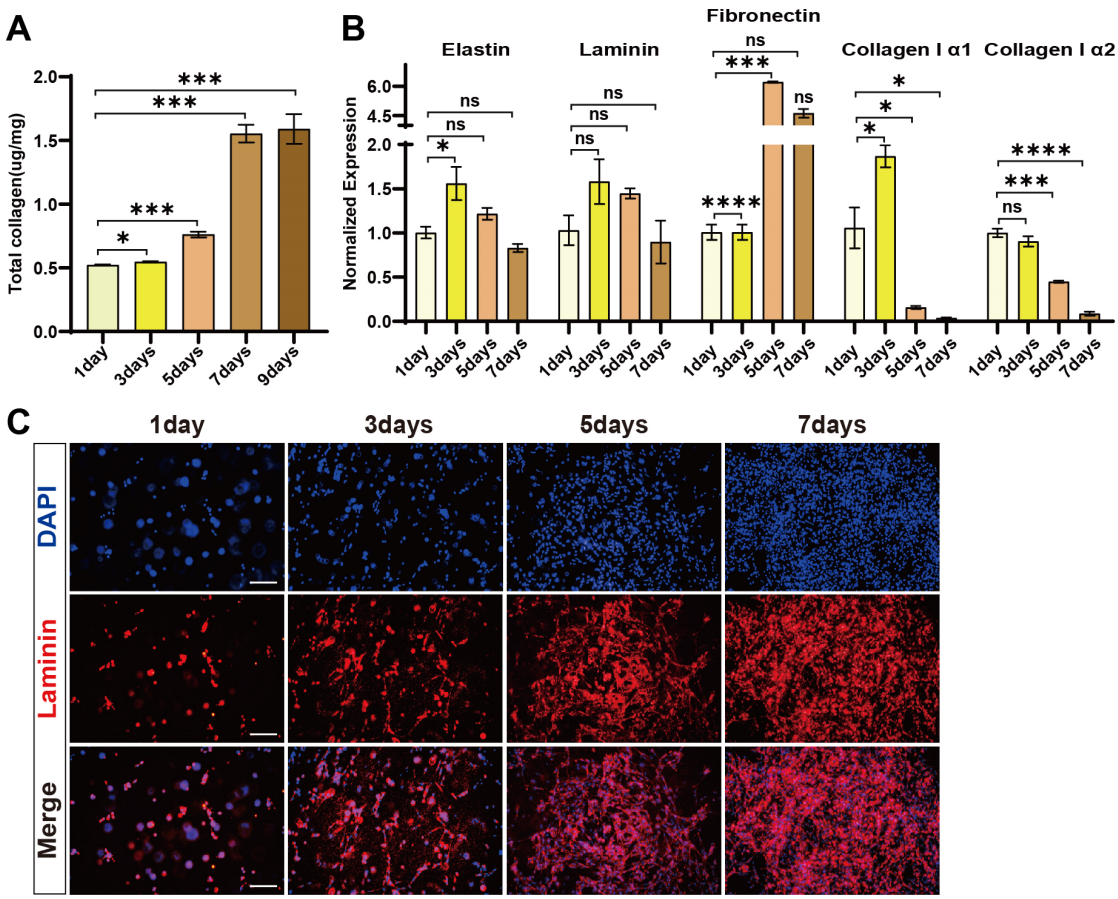

Figure 7. The collagen content and expression of ECM components in cultured meat. (A) Total collagen content of cultured meat at different days of cultivation. Error bars indicate s.e.m, n = 3. *P < 0.05, ***P < 0.001. (B) Expression of ECM-related genes determined by RT-qPCR of cultured meat. Error bars indicate s.e.m, n = 3. *P < 0.05, ***P < 0.001, ****P < 0.0001. (C) Representative Laminin staining of cells in 3D culture on 1day, 3days, 5days and 7days after cell implantation in hydrogel. Scale bar, 100 μm.

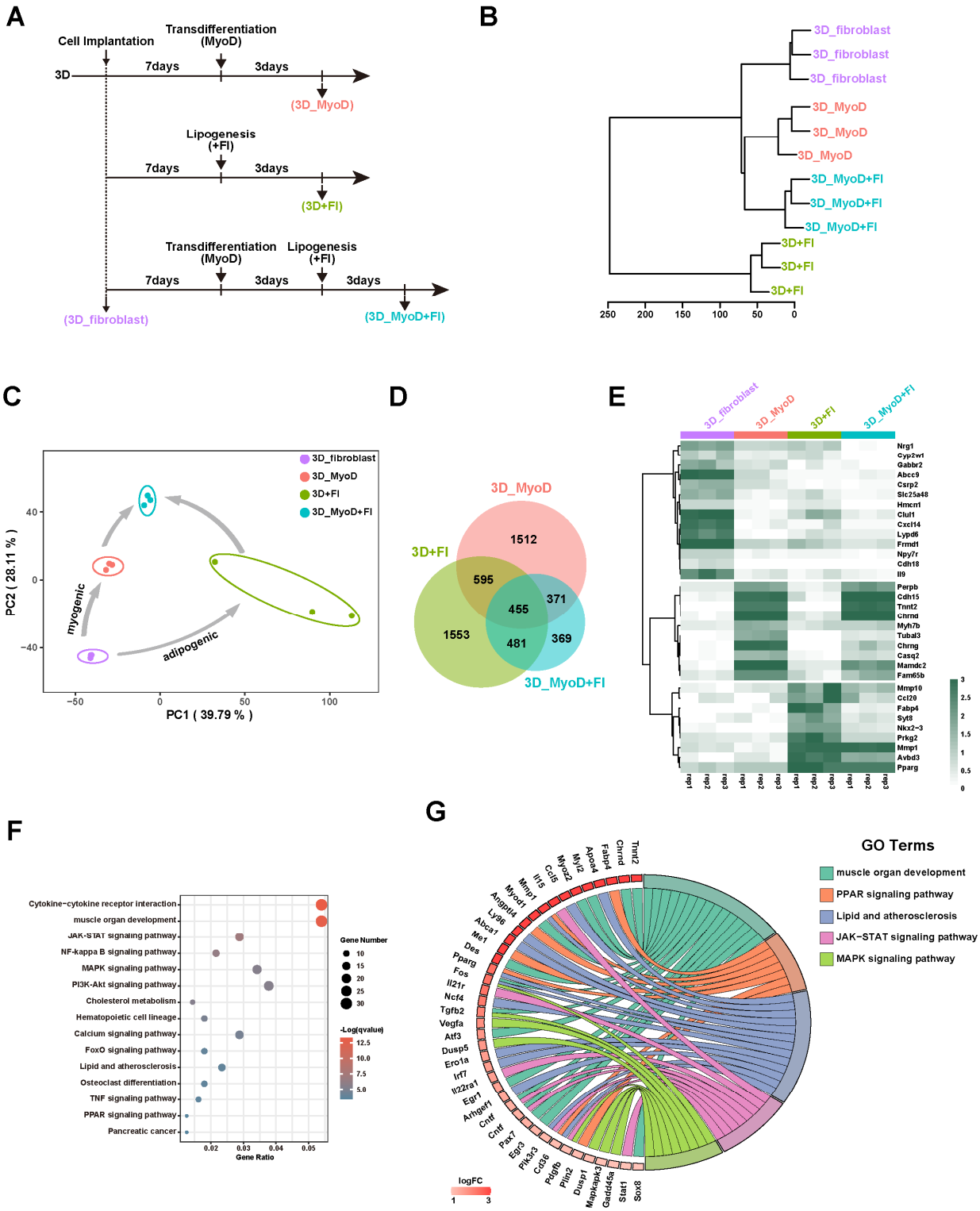
A
Cell Implantation
Transdifferentiation (MyoD)
3D
7days
3days
(3D_MyoD)
Lipogenesis (+FI)
7days
3days
(3D+FI)
Transdifferentiation (MyoD)
Lipogenesis (+FI)
7days
3days
3days
(3D_fibroblast)
(3D_MyoD+FI)
B
3D_fibroblast
3D_fibroblast
3D_fibroblast
3D_MyoD
3D_MyoD
3D_MyoD
3D_MyoD+FI
3D_MyoD+FI
3D_MyoD+FI
3D+FI
3D+FI
3D+FI
250
200
150
100
50
0
C
3D_fibroblast
3D_MyoD
3D+FI
3D_MyoD+FI
PC2 (28.11 %)
PC1 (39.79 %)
myogenic
adipogenic
D
3D_MyoD
3D+FI
3D_MyoD+FI
1512
595
371
455
1553
481
369
E
3D_fibroblast
3D_MyoD
3D+FI
3D_MyoD+FI
Nrg1
Cyp2w1
Gabbr2
Abcc9
Csrp2
Slc25a48
Hmcn1
Clut1
Cxcl14
Lypd6
Frmd1
Npy7r
Cdh18
Il9
Perpb
Cdh15
Tnnt2
Chrnd
Myh7b
Tubal3
Chrng
Casq2
Mamdc2
Fam65b
Mmp10
Ccl20
Fabp4
Syt8
Nkx2-3
Prkg2
Mmp1
Avbd3
Pparg
rep1
rep2
rep3
F
Cytokine-cytokine receptor interaction
muscle organ development
JAK-STAT signaling pathway
NF-kappa B signaling pathway
MAPK signaling pathway
PI3K-Akt signaling pathway
Cholesterol metabolism
Hematopoietic cell lineage
Calcium signaling pathway
FoxO signaling pathway
Lipid and atherosclerosis
Osteoclast differentiation
TNF signaling pathway
PPAR signaling pathway
Pancreatic cancer
Gene Ratio
Gene Number
-Log(qvalue)
G
GO Terms
muscle organ development
PPAR signaling pathway
Lipid and atherosclerosis
JAK-STAT signaling pathway
MAPK signaling pathway
logFC

951 **Figure 8.** Gene expression profiles during transdifferentiation and fat deposition in 3D.
952 (A) Scheme of the RNA-Seq samples marked by different color. (B) Hierarchical
953 clustering analysis of whole transcriptomes of 3D_fibroblasts, 3D_MyoD, 3D+FI, and
954 3D_MyoD+FI using Euclidean distance with ward.D cluster method. (C) PCA analysis
955 of transcriptome changes during myogenic transdifferentiation and fat deposition
956 (n= 10,247 genes). The ellipses group include three biological replicates in each cell
957 type. The arrows represent the wiring of gene expression under different conditions.
958 The routes were derived from original fibroblast toward two differentiation routes,
959 namely "myogenic transdifferentiation" and "adipogenic transdifferentiation". (D)
960 Venn Diagram showing the overlap of differentially expressed genes (DEG) from
961 3D_MyoD, 3D+FI, and 3D_MyoD+FI compared to the original 3D_fibroblasts. (E)
962 Heat map showed the representative genes differentially expressed between
963 3D_MyoD+FI and 3D_fibroblast cells (n=3 biologically independent samples). (F) GO
964 analysis of up-regulated DEGs between 3D_MyoD+FI vs. 3D_fibroblast cells. (G)
965 GOChord analysis of the up-regulated genes within representative pathway between
966 3D_MyoD+FI and 3D_fibroblast cells.